the confined dark space cavity imaging device, we completed the three-dimensional drawing and assembly of the monitoring imager parts through the SOLID WORKS2020 version, and performed explosion view operations on the completed parts to obtain simple equipment explosion drawings and equipment disassembly and installation animations, so that the structure can be more concise and convenient to understand, which is conducive to future production and installation. Understand the principle of rotating operation of the device, the determination of the measurement coordinate system and the coordinates of the origin, the measurement path planning, and carry out 360° data collection without dead angle through the motor drive and gear transmission of the device.

In the problem of selecting the best laser rangefinder, we comprehensively compare the laser rangefinders of five manufacturers, based on range, accuracy, price, and intuitively compare the cost performance of each rangefinder through curve fitting, so as to ensure the authenticity and reliability of project data and optimize the selection of laser rangefinders. In the end, it was decided to purchase a red laser rangefinder-keyence laser sensor with a detection distance of 60–5000 mm and a variable diameter of less than 40mm.

The system is equipped with an all-round automatic rotation device that can be equipped with a laser rangefinder, which can freely adjust the length of the robotic arm in extremely harsh environments that cannot be directly detected by artificially such as closed high temperature, and extend the laser rangefinder into the furnace, rotate in all directions according to the planned path, and automatically complete the measurement of the distance from the origin of the laser rangefinder to each point of the furnace. Therefore, compared with the manual detection of the mine furnace, this system can not only ensure the safety of the staff but also ensure the recovery of valuable energy in the furnace, reducing the cumbersome operation process and errors in manual calculation.

This project will develop a lightweight 3D reconstruction software and design a system based on laser ranging technology and grid imaging technology. Through the computer processing of the point data collected by the laser rangefinder real-time imaging and three-dimensional reconstruction, constitute a closed inner cavity shape, and then carry out data analysis, at the same time the user can operate the canvas to zoom in, zoom in, translate and rotate, etc., clearly and clearly observe the structure of the inner cavity of the mineral heating furnace.

In the processing of point data, we chose B-spline curves with excellent properties such as geometric invariance, convexity, convexity, variation reduction, and local support. Although the least squares method is simple and easy to implement, if the fitting mode is not selected properly, it will produce a large deviation.

This system and device are widely used and universal. The project concept is derived from common problems in industrial production, and the results obtained by the experiment can be widely used in various fields and can significantly improve its work efficiency.

References

1. Basic parameters in the operation and design of submerged arc furnaces, with particular reference to production of high-silicon alloys[J]. Journal of the Southern African Institute of Mining and Metallurgy,2018,118(6).

УДК: 69.003.13

赤泥联合钢渣的铁铝分离技术

孙悦（Sun Yue）
东北大学（Northeastern University）
e-mail:2671733743@qq.com

Summary. *This project provides the theoretical and experimental basis for the industrial production of Weiqiao alumina red mud, and at the same time fundamentally solves a series of problems such as waste of resources, environmental pollution and storage costs caused by red mud stockpiling, so as to truly achieve sustainable economic development.*

The experimental raw materials were Weiqiao red mud, steel slag, bauxite and anthracite. The red mud used in the experiment was taken from Shandong Weiqiao alumina plant, and the steel slag was from the leaching slag of the experimental process, and the chemical composition of the red mud is shown in tab.1.The typical composition of slag for different processes in steelmaking. The main physical phases of slag include β-C_2S, C_2MS_2, C2F, FeO, MgO, CaO, Fe_2O_3 and a small amount of pure iron.

Ingredients	Bayer	Sintered	Joint Law	Weiqiao
Fe_2O_3	30～60	7～10	6.1～7.5	56.0486
Al_2O_3	10～20	5～7	5.4～7.5	23.1948
SiO_2	20～31	20～30	20.0～20.5	8.7290
TiO_2	Trace～10	2.5～3.6	6.1～7.7	7.3271
CaO	2～8	46～49	43.7～46.8	2.7468
Na_2O	—	—	—	0.6966
MgO	—	1.2～1.6	—	0.1421
K_2O	—	0.2～2.4	0.5～0.7	0.0781

Figure 1 – Chemical composition content (mass fraction) of the red mud produced by the three processes and Weiqiao

The red mud, steel slag, bauxite and anthracite were crushed, ground through a 200 mesh (75 μm) sieve, dried and prepared for use.The raw ore is reduced in a slag bath under high temperature conditions, and the iron concentrate is obtained by magnetic separation, and the Al element is recovered by alkali leaching. The process includes 3 steps of slag bath reduction, magnetic separation and alkali leaching.

The raw material ore was made by mixing steel slag, red mud, bauxite and anthracite in the ratio of 30:24:15:2, 88:40:33:6, 25:12:15:2, 53:48:32:4 by mass. The raw material ore was put into a graphite crucible and placed in a melt reactor and held at a temperature of 1500 °C for 1 hour, while the material was then allowed to cool with the furnace using the 5 °C cooling method, and the cooled material was removed to obtain the upper layer of calcium aluminate slag and the lower layer of iron ingots.

The samples were placed in a fluid magnetic separator and separated by magnetic separation at a magnetic field strength of 1.59×105 A-1m-1 to obtain magnetic and non-magnetic phases, and the pig iron was analyzed for composition, the iron recovery was calculated, and the iron grade values were determined by microwave digestion.

For the aluminum slag obtained from the slag bath reduction, alkali leaching was performed with Na_2CO_3 solution, and the ground finished calcium aluminate slag was leached by magnetic stirring, and the leached slurry was filtered and washed by liquid-solid separation through a filter extractor, while the dissolved slag was placed in a muffle furnace for drying afterwards.

$Fe_2O_3 + CO \rightarrow 2FeO + CO_2$

$Fe_2O_3 + 3CO \rightarrow 2Fe + 3CO_2$

$Fe_3O_4 + CO \rightarrow 3FeO + CO_2$

$2FeO + C \rightarrow 2Fe + CO_2\uparrow$

$FeO + CO \rightarrow Fe + CO_2$

The process of aluminum dissolution reaction:

$CaO \cdot Al_2O_3 + Na_2CO_3 + 4H_2O \rightarrow 2NaAl(OH)_4 + CaCO_3\downarrow$

$CaO \cdot 2Al_2O_3 + 2Na_2CO_3 + 8H_2O \rightarrow 4NaAl(OH)_4 + CaCO_3\downarrow + CO_2\uparrow$

$12CaO \cdot 7Al_2O_3 + 12Na_2CO_3 + 33H_2O \rightarrow 14NaAl(OH)_4 + 12CaCO_3\downarrow + 10NaOH$

$2CaO \cdot SiO_2 + 2Na_2CO_3 \rightarrow 2CaCO_3\downarrow + Na_2SiO_3 + 2NaOH$

$1.7Na_2SiO_3 + 2NaAl(OH)_4 \rightarrow Na_20 \cdot Al_2O_3 \cdot 1.7SiO_2 \cdot nH_2O\downarrow + 3.4NaOH$

From the analysis in tab. 2 , the aluminum dissolution rate reached the highest value of 73.5 % in the present data at the material mass ratio of steel slag: red mud: bauxite: anthracite = 25:12:15:2. The iron reduction rate reached more than 80 % under all four groups of material ratios.

Material Serial number		Steel slag	Red mud	Bauxite	Anthracite	Aluminum dissolution rate	Iron reduction rate
Quality ratio	1	30	24	15	2	71.1	Basically above 80%
	2	88	40	33	6	65.4	
	3	25	12	15	2	73.5	
	4	53	48	32	4	69.8	

Figure 2 – Relationship between the mass ratio of materials and the reduction rate of aluminum and iron

УДК 69.003.13

WTHERMOTUBE – NEW HIGH EFFICIENCY AND ENERGY SAVING HEAT DISSIPATION SYSTEM FOR DATA CENTER

谭越中 (Yuezhong Tan), 余茂椿 (Maochun Yu),
崔学荣 (Xuerong Cui), 李宗海 (Zonghai Li)
东北大学（Northeastern University）
e-mail: tyz20011113@163.com

Summary. *Our passive refrigeration technology has been continuously studied, and a number of core technologies using gravity heat pipes for heat dissipation have been put forward. Through the phase change of working medium, efficient heat dissipation can be realized with very little energy consumption, and the working efficiency is extremely high.*

Nowadays, the heating density of data center is increasing rapidly, and the equipment used to solve the heat dissipation problem also consumes huge energy. Therefore, we designed a data center refrigeration and heat dissipation optimization system, which greatly improved the heat dissipation capacity and energy utilization efficiency of the data center. We build this system through eight high-level papers, four patents and six soft works.

The heat dissipation envelope designed by us embeds gravity heat pipe array into the wall, the evaporation section of the heat pipe is located at the lower part of the inner surface of the wall, and the condensation section is located at the upper part of the outer surface of the wall. The working medium in the heat pipe can evaporate under the drive of temperature difference and return under the action of gravity, which can transfer heat efficiently without additional power input. The structural unit is shown in fig. 1.

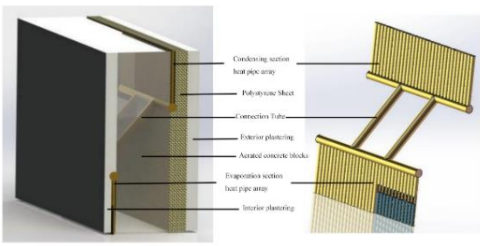

Figure 1 – Control diagram of heat pipe embedded

The structure of the device comprises a chassis containing double capillary short tubes embedded with chips and gravity heat pipes, wherein the evaporation section and condensation section of the gravity heat pipe are respectively connected to the capillary short tubes and the shell of the chassis, the chip is provided with a swing structure, and a direct evaporative cooler is arranged between the chassis and the wall. The physical diagram and structure diagram are shown in fig. 2, and the heat energy flow direction is shown in fig. 3.